X62-10889

TECHNICAL MEMORANDUM

X-699

PRELIMINARY RESULTS ON HEAT TRANSFER TO THE AFTERBODY OF THE APOLLO REENTRY CONFIGURATION

AT A MACH NUMBER OF 8

By Robert A. Jones

Langley Research Center
Langley Station, Hampton, Va.

NATIONAL AERONAUTICS AND SPACE ADMINISTRATION

WASHINGTON   September 1962

DECLASSIFIED

CONFIDENTIAL

NATIONAL AERONAUTICS AND SPACE ADMINISTRATION

TECHNICAL MEMORANDUM X-699

PRELIMINARY RESULTS ON HEAT TRANSFER TO THE AFTERBODY OF

THE APOLLO REENTRY CONFIGURATION

AT A MACH NUMBER OF 8*

By Robert A. Jones

SUMMARY

Heat-transfer rates on the afterbody of the Apollo reentry configuration have been measured in a low-enthalpy wind tunnel at a Mach number of 8. The data have been presented as the ratio of the measured heat-transfer coefficient on the afterbody to the calculated heat-transfer coefficient at the stagnation point at zero angle of attack. This ratio was found to vary from a low of approximately 0.01 to a maximum of about 0.52 as the angle of attack varied from $0°$ to $55°$.

INTRODUCTION

The heat-transfer distribution on the afterbody of the Apollo reentry vehicle is at present one of the largest unknown factors affecting the design. A rather extensive investigation to determine the importance of various parameters on heating in this region is now in progress. It is the purpose of this report to make available some of the data already obtained. These data were taken in the Langley Mach 8 variable-density tunnel at a low-enthalpy (350 Btu/lb) at free-stream Reynolds numbers of 0.06×10^6 to 1.36×10^6 based on body diameter.

SYMBOLS

c   specific heat of wall

c_p specific heat of air at constant pressure

*Title, Unclassified.

D   diameter

h   heat-transfer coefficient, $\dfrac{\rho c \tau \frac{dT_W}{dt}}{T_O - T_W}$

l afterbody length (fig. 1)

N_{Pr} Prandtl number

r_c radius at corner

r_n radius at nose

r_r radius at rear

R   free-stream Reynolds number based on maximum body diameter

s   surface distance measured from stagnation point (fig. 1)

t   time

T   temperature

V   velocity at edge of boundary layer

x   distance along afterbody measured from tangent point of forward corner and afterbody (fig. 1)

α angle of attack

μ viscosity

ϕ angle of roll

ρ density

τ skin thickness

Subscripts:

o   free-stream stagnation condition

s   stagnation conditions behind normal shock at zero angle of attack

w   at wall

TEST FACILITY

These tests were conducted in the Langley Mach 8 variable-density tunnel; the tunnel is described in reference 1. This tunnel has an axisymmetric contoured nozzle terminating in an 18-inch-diameter test section. Stagnation pressures used were approximately 30, 100, 300, and 1,000 pounds per square inch absolute with stagnation temperatures from 700° F to $1,000^{\circ}$ F, depending on the pressure. The nominal Mach number in the test area was 7.95 ± 0.05 for stagnation pressures higher than 100 pounds per square inch absolute. The tunnel has not been calibrated at pressures lower than this.

Model

The model (fig. 1) was constructed from AISI Type No. 347 stainless steel. The thin-walled shell had a nominal thickness of 0.025 inch. The actual thickness varied ± 0.005 inch, and therefore measurements accurate to ± 0.0005 inch were made at each thermocouple location. Thermocouples were made from AWG No. 30 iron-constantan wire and spot welded to the inner surface of the shell in three rows of seven each at $\phi = 0^{\circ}$, 45°, and 90°. (See fig. 1.) The leads were brought out through the center of the sting. This sting was sharpened on both the leading and trailing edge so as to disturb the flow as little as possible. The two stings shown in figure 1 were identical except for the angle which they made with the center line of the model.

TEST TECHNIQUE AND DATA REDUCTION

Data were obtained by using a transient testing technique. The tunnel was started and brought to the desired operating conditions, and then the model was rapidly injected into the airstream by a pneumatic piston. The time required for the model to pass through the tunnel boundary layer and for steady flow over the model to be established was about 0.05 second. The thermocouple outputs were recorded 40 times per second by a Beckman 210 high-speed analog to digital data recording system. Heat-transfer coefficients were obtained by fitting a second-degree curve to the temperature-time data by the method of least squares and computing the time derivative of temperature on a card-programed computer. The heat-transfer coefficient is given by the equation

$$h = \frac{\rho c \tau \dfrac{dT_w}{dt}}{T_O - T_w} \tag{1}$$

For these tests, heat-transfer coefficients were computed for the time interval from 0.1 to 1.0 second after injection of the model into the airstream. These short times together with temperature-rise rates of 20° per second or less resulted in a nearly isothermal surface. The conduction along the thin skin of the model was therefore thought to be negligible. A more complete description of this test technique and the data reduction method is given in references 1 and 2.

A recovery factor of 1 was assumed in determining the temperature potential $T_O - T_W$ of equation (1). No attempt was made to measure the actual recovery factor. However, a calculation was made to estimate the effect of recovery factor on the data. Assuming a recovery factor of 0.85 and isentropic expansion from stagnation conditions behind the normal shock to free-stream static pressure indicated that the resulting difference in h would be only 10 percent.

The data are presented as the heat-transfer coefficient ratio h/h_s where h is the measured local value and h_s is the theoretical value for the stagnation point at zero angle of attack. The value of h_s was computed by the method of reference 3 (assuming a Lewis number of 1):

$$h_s = 0.768 \frac{c_p}{778} \left(N_{Pr,w}\right)^{-0.6} \left(\rho_w \mu_w\right)^{0.10} \left(\rho_s \mu_s\right)^{0.40} \left(\frac{dV}{ds}\right)^{1/2} \qquad (2)$$

where dV/ds was determined from reference 4 and found to be 1.19 times the value of the Newtonian velocity gradient of a sphere of radius r_n. All the data presented herein were obtained with sting 1. Data taken with sting 2 at an angle of attack of 35° indicated that changing stings had essentially no effect on the heat-transfer distribution at the higher angles of attack. However, there may have been some sting-interference effects at low angles of attack, particularly at zero.

RESULTS AND DISCUSSION

The variation of the heat-transfer coefficient ratio with distance along the windward ray of the afterbody (measured from the tangent point of the forward corner and afterbody) is shown in figure 2. Values of h_s used for each free-stream Reynolds number are also given in figure 2. Note the change in heat-transfer distribution with angle of attack. At angles of attack of 0° and 5°, the heating increased somewhat with distance, while at 15° and 25° it was almost constant, and at higher angles of attack it decreased with distance. The cause for the rapid increase

in heat transfer with distance from the corner at the high Reynolds number (136×10^4) and zero angle of attack was not known. Additional tests will be necessary to clarify this phenomenon.

For angles of attack of 25° and less, the maximum rate of heat transfer to the afterbody was always less than 10 percent of that at the stagnation point at zero angle of attack; however, at a 55° angle of attack it was as high as 52 percent of the value at the stagnation point at zero angle of attack. At this angle the windward ray of the afterbody was inclined 20° into the wind.

The distribution of heat transfer around the afterbody is shown in figure 3 for x/l of 0.402. There was a rather rapid decrease in heating rate with angular distance from the windward ray, particularly at the high angles of attack.

Schlieren photographs of the flow about the model are shown in figure 4. For these photographs, the knife edge was horizontal. Note that the sting had virtually no effect on the shape of the shock wave. Also note how the shock-detachment distance became smaller near the corner at high angles of attack.

CONCLUDING REMARKS

Preliminary results on the heat transfer to the afterbody of the Apollo reentry configuration at a Mach number of 8 indicate that the ratio of the measured heat-transfer coefficient on the afterbody to the calculated heat-transfer coefficient at the stagnation point at zero angle of attack varied from a low of 0.01 to a maximum of about 0.52 as the angle of attack varied from 0° to 55°. These results also indicate that at the higher angles of attack there was a rather rapid decrease in heating rate with angular distance away from the windward ray.

Langley Research Center,
National Aeronautics and Space Administration,
Langley Station, Hampton, Va., May 15, 1962.

CONFIDENTIAL

REFERENCES

1. Jones, R. A.: Heat-Transfer and Pressure Distributions on a Flat-Face Rounded-Corner Body of Revolution With and Without a Flap at a Mach Number of 8. NASA TM X-703, 1962.

2. Jones, Robert A., and Gallagher, James J.: Heat-Transfer and Pressure Distributions of a 60° Swept Delta Wing With Dihedral at a Mach Number of 6 and Angles of Attack From 0° to 52°. NASA TM X-544, 1961.

3. Fay, J. A., and Riddell, F. R.: Theory of Stagnation Point Heat Transfer in Dissociated Air. Jour. Aero. Sci., vol 25, no. 2, Feb. 1958, pp. 73-85, 121.

4. Boison, J. Christopher, and Curtiss, Howard A.: An Experimental Investigation of Blunt Body Stagnation Point Velocity Gradient. ARS Jour., vol. 29, no. 2, Feb. 1959, pp. 130-135.

L
3
0
3
1

CONFIDENTIAL

D = 4.00 inch

ϕ

$\frac{3}{8}$

Rear view

$r_n = 1.200\ D$
$r_r = 0.0918\ D$
$r_c = 0.050\ D$
$l = 0.700\ D$

Sting 2

Thin walled shell screwed and silver-soldered to body

$r_{r'}$

35°

r_n

r_c

S

D

Sting 1

Side view
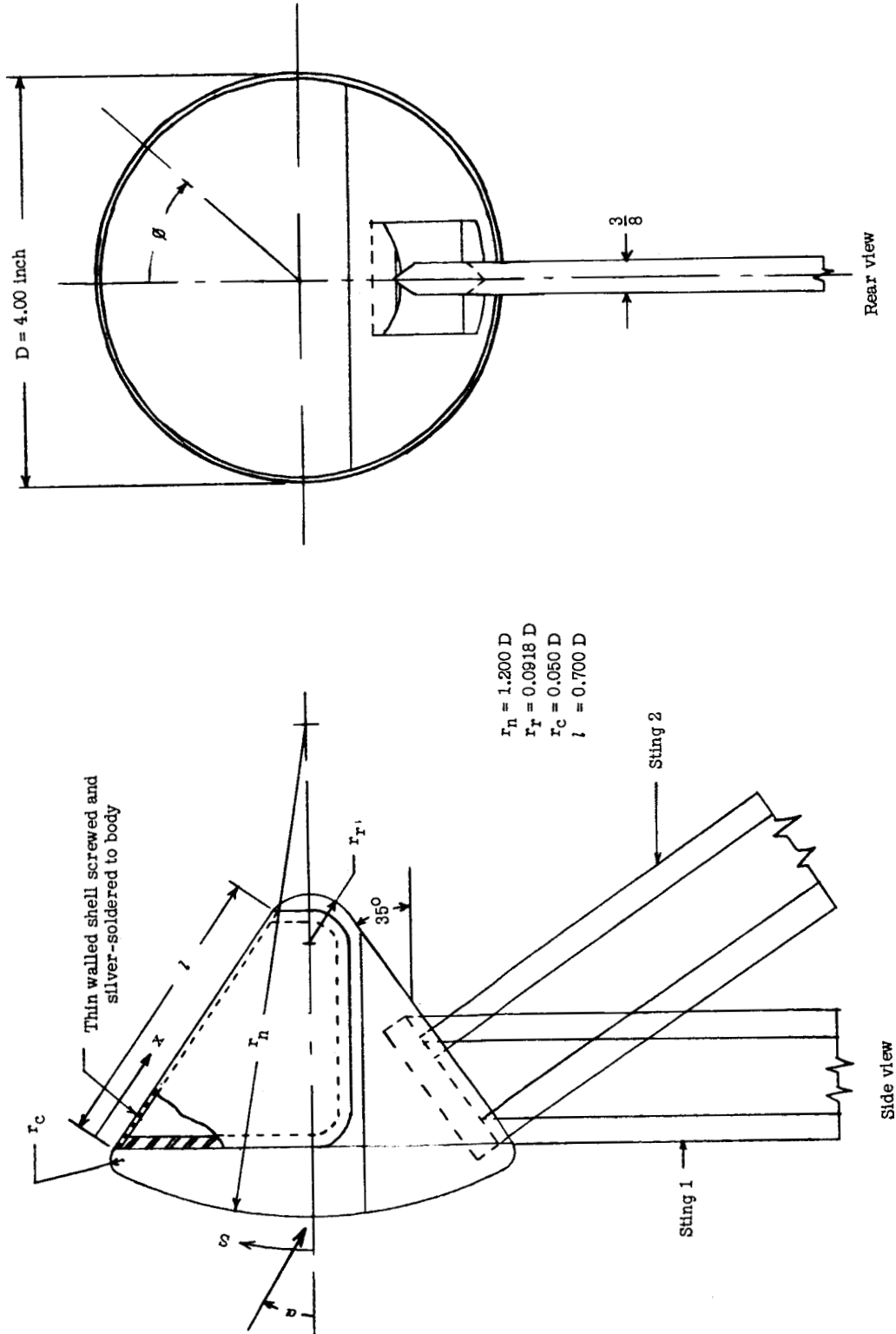
Figure 1.- Sketch of model.
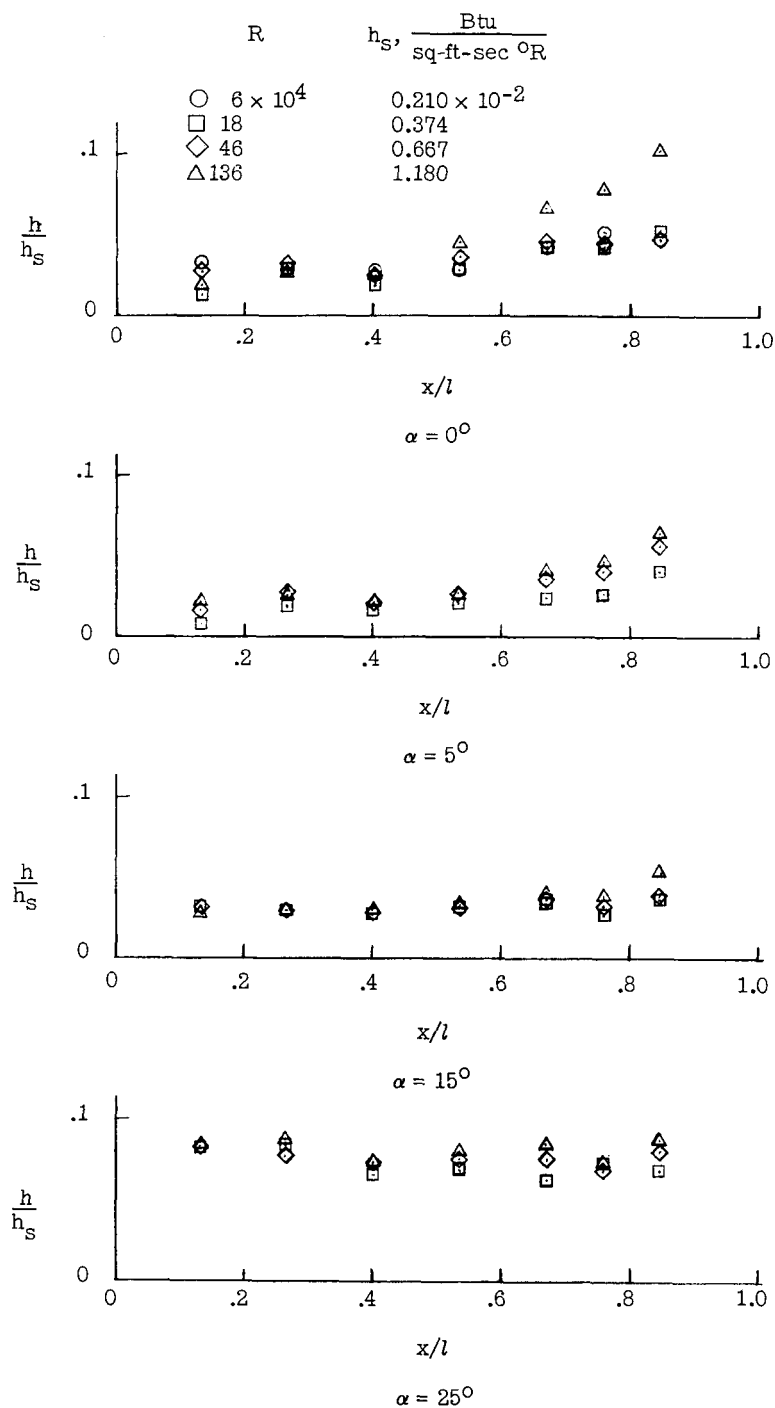
(a) $0° \leqq \alpha \leqq 25°$.

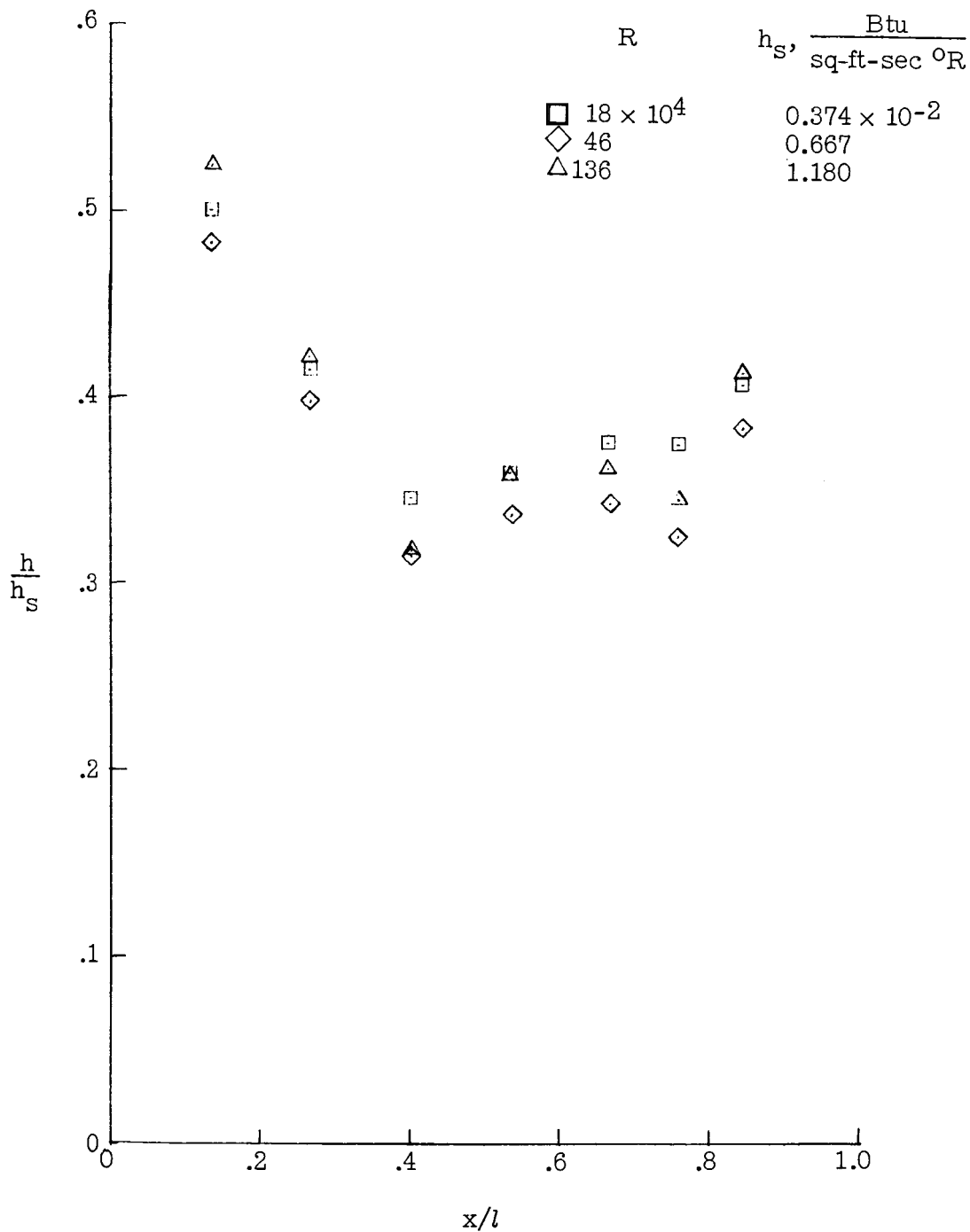Figure 2.- Variation of heat transfer along windward ray of afterbody.

CONFIDENTIAL

(b) $\alpha = 35°$.

(c) $\alpha = 45°$.

Figure 2.- Continued.

R	h_s, $\dfrac{Btu}{sq\text{-}ft\text{-}sec\ ^oR}$
□ 18×10^4	0.374×10^{-2}
◇ 46	0.667
△ 136	1.180

$\dfrac{h}{h_s}$

x/l

(d) $\alpha = 55^o$.
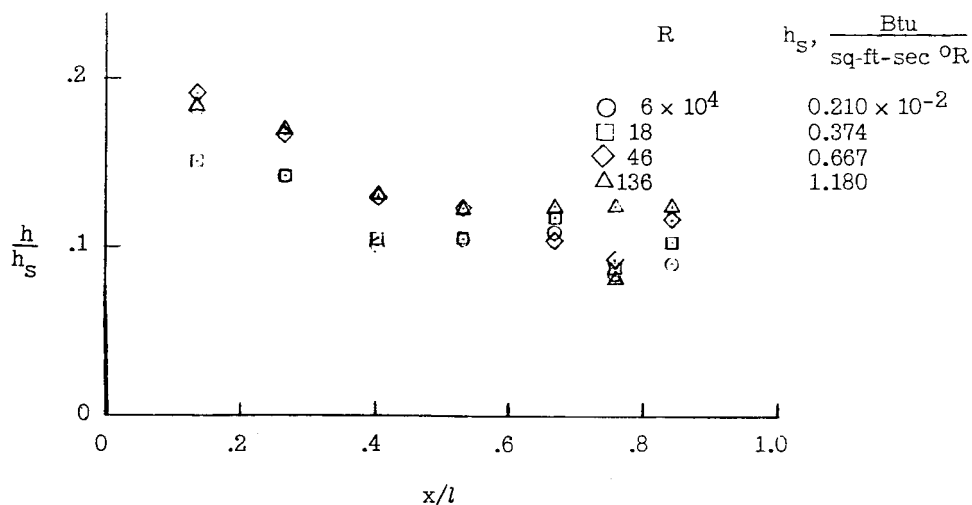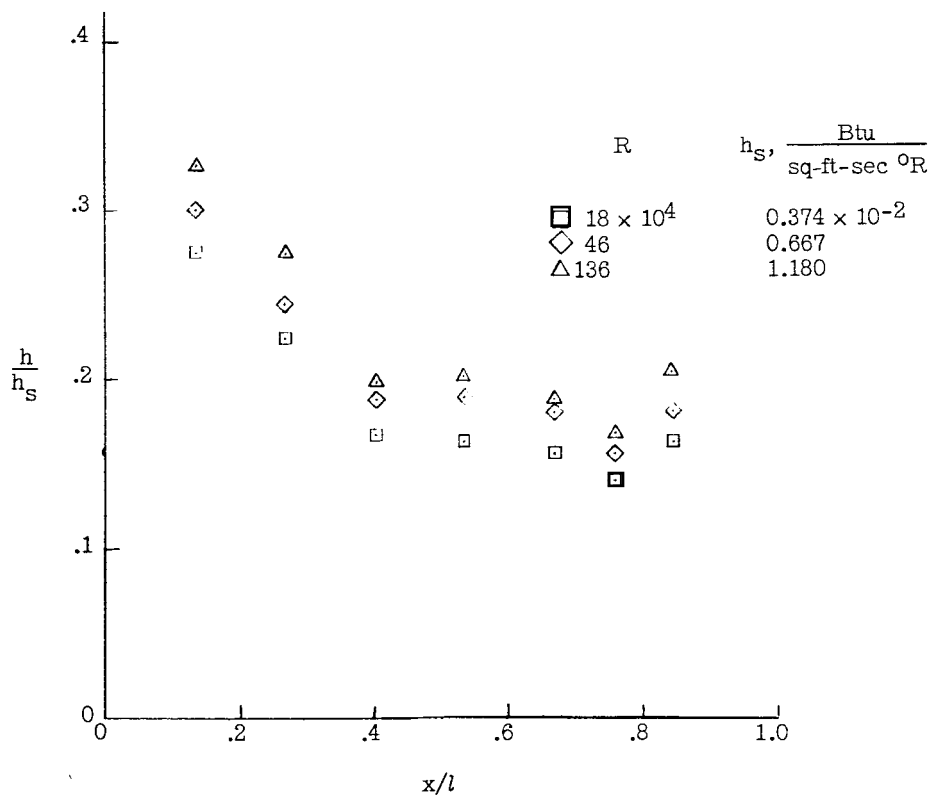
Figure 2.- Concluded.
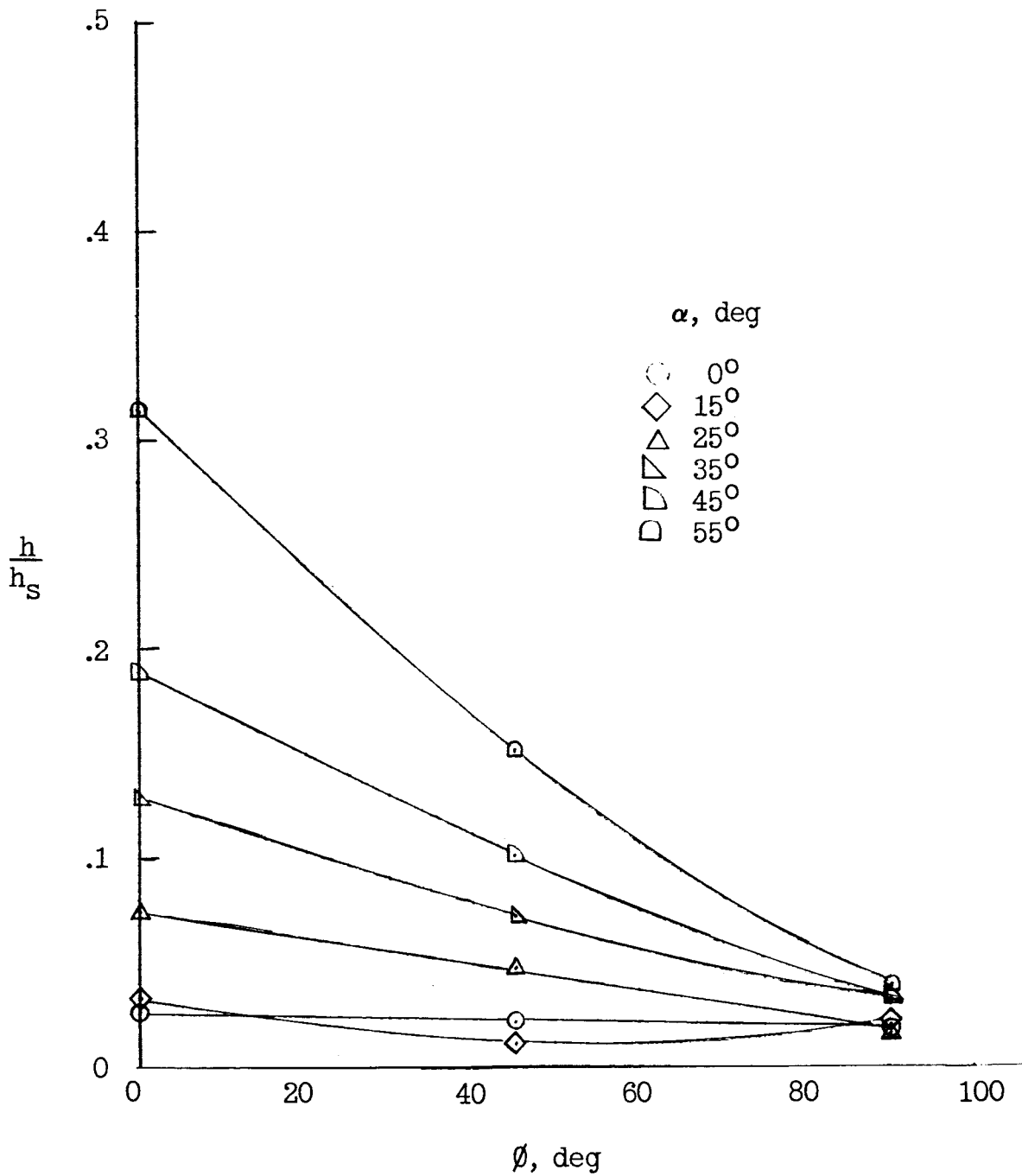
L-3031

Figure 3.- Variation of heat transfer around afterbody $(x/l = 0.402)$.
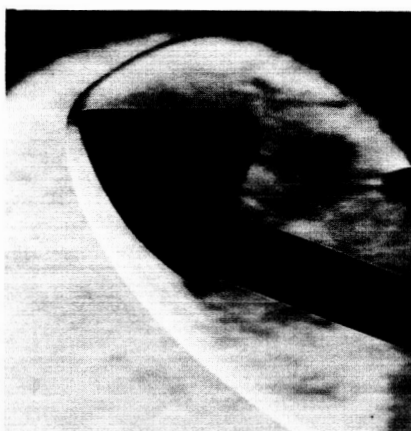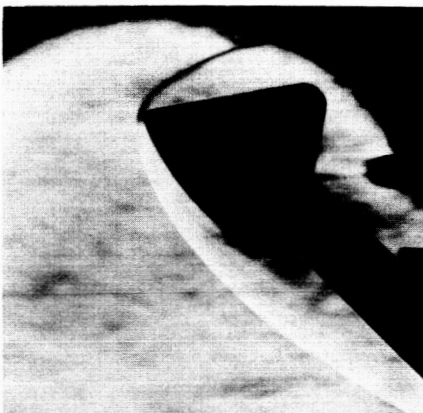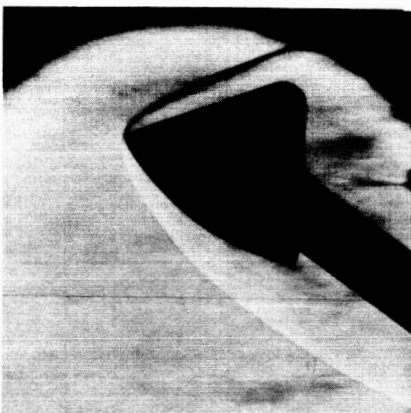$R = 46 \times 10^4$.

CONFIDENTIAL
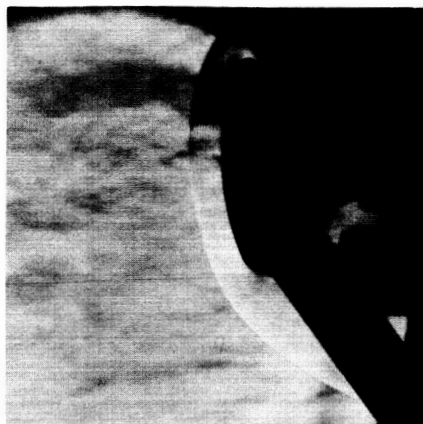
$\alpha = 0^{\circ}$
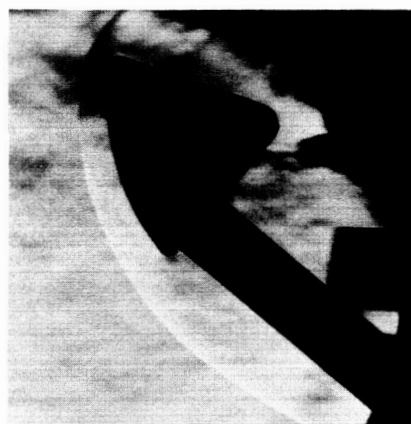
$\alpha = 15^{\circ}$
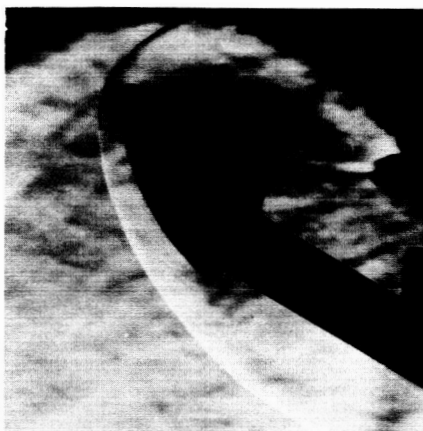
$\alpha = 25^{\circ}$

$\alpha = 35^{\circ}$

$\alpha = 45^{\circ}$

$\alpha = 55^{\circ}$

Figure 4.- Schlieren photographs.   L-62-2058

CONFIDENTIAL